Journal of Engineering and Applied Sciences 13 (24): 10334-10348, 2018
ISSN: 1816-949X

Experimental and Numerical Study of Two Phase Flow (Air-Water) in Ribs Divergent Rectangular Duct

[1]Abbas Sahi shareef, [2]Riyadh S. Al-Turaihi and [1]Ali Abdalaimma
[1]Department of Mechanical Engineering, University of Kerbala, Kerbala, Iraq
[2]Department of Mechanical Engineering, University of Babylon, Hilla, Iraq

Abstract: An experimental and numerical study is carried out of two-phase flow phenomena in a divergence ribs rectangular duct for two positions: vertical and inclined (65° with horizontal) with two opening divergence angles. The experiments are performed in the duct with the water-air flow with various water and air discharges. The purpose of the these study to visualize the two phase flow phenomena in addition to studying the effect of the pressure difference through the divergence. All the experimental data in this study are achieved by utilizing a pressure sensor and imagined by a video camera for various water discharges (5, 15 and 20 L/min), various air discharges (8.333, 10.833 and 16,666 L/min) and the opening angles are 10 and 15°. The results show that when the opening divergence angle increases from (10-15) at constant air and water discharge, the pressure recovery through the divergence ribs rectangular duct section decreases by 11%.

Key words: Two-phase flow, divergence ribs rectangular duct, opening divergence angle, difference, recovery, phenomena

INTRODUCTION

Two-phase flow is defined as two-phase flow simultaneously in the same pipe, like gas and liquid, gas and solid, two dissimilar liquids or liquid and solid. The most complex of these types is the flow of gas liquids due to the compressibility and deformation of both phases. Two-phase flow can be often met in chemical or mechanical engineering applications, oil wells, power generation, reactors, boilers, condensers, evaporators and combustion systems. Usually, valves exist in transporter pipes for vapor and water in a steam turbine or boiler. These valves are geometrical singularities as divergence or convergence which may greatly affect the behavior of two-phase flow including pressure change, void fraction distribution and flow pattern. Therefore, specific study is a significant issue when the application interests industrial safety valves. There are numerous studies of two-phase flow in channels with the constant area, however, in contrast to the studies of two-phase flow in divergence, there are somewhat few studies of convergence, divergence, bends and other types of singularities. It is necessary to study this geometry for knowing its effect on the distribution of pressure and flow patterns and thus get the best design of the system. Due to its industrial significance, The two-phase flow in the expansion sections was studied widely by researchers. Kondo *et al.* (2002) investigated the air-water vertical flow in a circular tube with an axisymmetric sudden enlargement. Due to high shear stress produced directly above the enlargement, distortion of the bubble and breakage of the slug was occurred. Ahmed *et al.* (2007) established a general formulation, depended on a sequence of an experiment on air-oil horizontal flow through sudden enlargements, for the losses in recirculation zone and void fraction changes and pressure recovery across the sudden enlargement due to the wall shear stress. Chen *et al.* (2007) studied the air-water flow pattern of a sudden enlargement in a small rectangular duct. A new liquid-jet flow pattern was appear for low quality which decreases the pressure change across the area enlargement. Ahmed *et al.* (2008) experimental investigate characterizes the progress of air-oil flow downstream of sudden expansions. The results showed that the void fraction increased as the flow approached the sudden expansion, due to separation of air in the recirculation region. The oil turbulence amount was larger in the nearness of the sudden expansion. Air-water flows through smooth enlargements were investigated carefully by Kourakos *et al.* (2009) and Wang *et al.* (2010) were offered a complete estimation of available pressure relationships for the two-phase flow. Abadie *et al.* (2012) results demonstrated that the length of the bubble and slug rises when the flow rate ratio of liquid and gas rises,

Corresponding Author: Abbas Sahi shareef, Department of Mechanical Engineering, University of Kerbala, Kerbala, Iraq

the and a modified relationship was provided for ΔP. Anupriya and Jayanti (2014) studied air-water flow in an enlargement study. It was shown that recovery of pressure directly after enlargement is influenced by the interfacial friction and smoothness of the enlargement. For sudden enlargement restrictions in small ducts, the values of pressure drop, the two-phase empirical relationships and flow pattern were mentions by Abdelall *et al*. (2005), Chen *et al*. (2008). As for numerical studies Abed and Al-Turaihi (2013) a two-phase (air-water) flow study was carried out through an inclined pipe with 30° with the horizontal. A camera was used to analyze the images and sensors were used to measure the pressure. It was concluded that the flow pattern depended on the air and water velocity. As it was observed that the pressure decreased with length the pipe when increasing the velocity of air and water (Brankovic and Currie, 1996) utilizing a Lagrangian approach for a gas bubble while for liquid flow, Eulerian approach was used. Behzadi *et al*. (2004) improved the Eulerian approach for two-phase flow (bubble flow) with a high void fraction. A bubble flow simulator was also, performed successfully through a sudden divergent study. Roul and Dash (2011) employed the Eulerian-Eulerian approach with turbulent model kepsilon, the results show the numerical values for pressure difference across sudden enlargement was good agreement with experimental values. It was also concluded that the mixture model is better than the homogeneous model to obtain an acceptable numerical simulation. Sakr *et al*. (2012) used SST (k-ω) turbulent model for a numerical simulation. It was found that this model gives accurate results for two-phase flow across the sudden enlargement. Eskin and Deniz (2012) the Eulerian approach was used with RMS turbulent model for two-phase flow through sudden enlargement. It was observed that the deviation between the numerical values of void fraction and the pressure difference with the experimental values was increased with the increase of the void fraction. Ueda *et al*. (2012) used the volume of fluid VOF model which includes the effect of wall adhesion and surface tension on flow, it was successfully predicted for the bubble flow pattern for low gas discharge and annular flow pattern for high gas discharge. Ahmadpour *et al*. (2016) conducted a numerical simulation for the two-phase flow (water-air) through divergence/convergence of constant opening angles; the k-ε turbulence model was used. The results obtained were compared with previous surveys. The effect of void fraction, opening angle and Reynolds number was studied on pressure distribution inside a test channel this research, an experimental and numerical study of two-phase flow was carried out across a gradual divergent section. The effect of increasing the discharge of air and water and increasing the angle of divergent to recovery pressure through this study.

MATERIALS AND METHODS

Experimental setup: An experimental rig was constructed to study the two-phase flow phenomena inside a divergence ribs rectangular duct. The equipment used for the experimental test and the measuring system is illustrated in Fig. 1a, b. Two test sections were used with an opening angle of 10 and 15° as illustrated in Fig. 2. The cross-section area of the bottom surface of test sections was 2*6 and the length was 0.5 m long while the section area of top surface was 2*8 cm with a length of 0.5 m. The material of the test section was a perspex sheet with a thickness of 1 cm. The divergence section has four ribs, two ribs on each side with dimensions 0.5*0.5*2 cm. The purpose of these ribs is to create strong turbulence intensity inside the divergence section by breaking the laminar-sub layer leading to rapid mixing between the phases. The experimental rig equipment consists of the following:

Water reservoir of capacity 500 L. Water pump with discharges (5-480) L/min, head (5-20) m, Power (1.5 kW) and 1410 rpm. Valves and piping system for water (1.25) in. Water flow meter was utilized to measure the discharge of water entered in the test section with range 5-35 L\min. Air compressor was utilized for air processing with a specification of a capacity (0.5 m^3) and a maximum pressure of (16 bar). Air flow meter was utilized for measuring the discharge of air that enters the test channel with a range of (5.833-58.33 L/min). Valves and piping system for air (0.5) in. Pressure sensors which were utilized to measure the pressure field with a range of (0-1 bar) and these pressure sensors were distributed along the test channel with an accuracy of (0.1%).

An interface was utilized to connect the pressure sensor to a personal computer. The interface converts the voltage (analog) signal from the pressure sensors into a digital signal that can be read through a software program (DaLi08) run on the personal computer. A universal data logger (UDL100) was used. It had high accuracy and resolution, the sampling period (750 msec) and channel isolation voltage of (400 V). A Sony digital camera of DSC-W220 Model used to show the behavior of the two phase flow through a channel.

Experimmental procedure: After building the system and installing all the measuring devices, the system was operated several times to confirm that there was no leak or any operating mistakes. During this research,

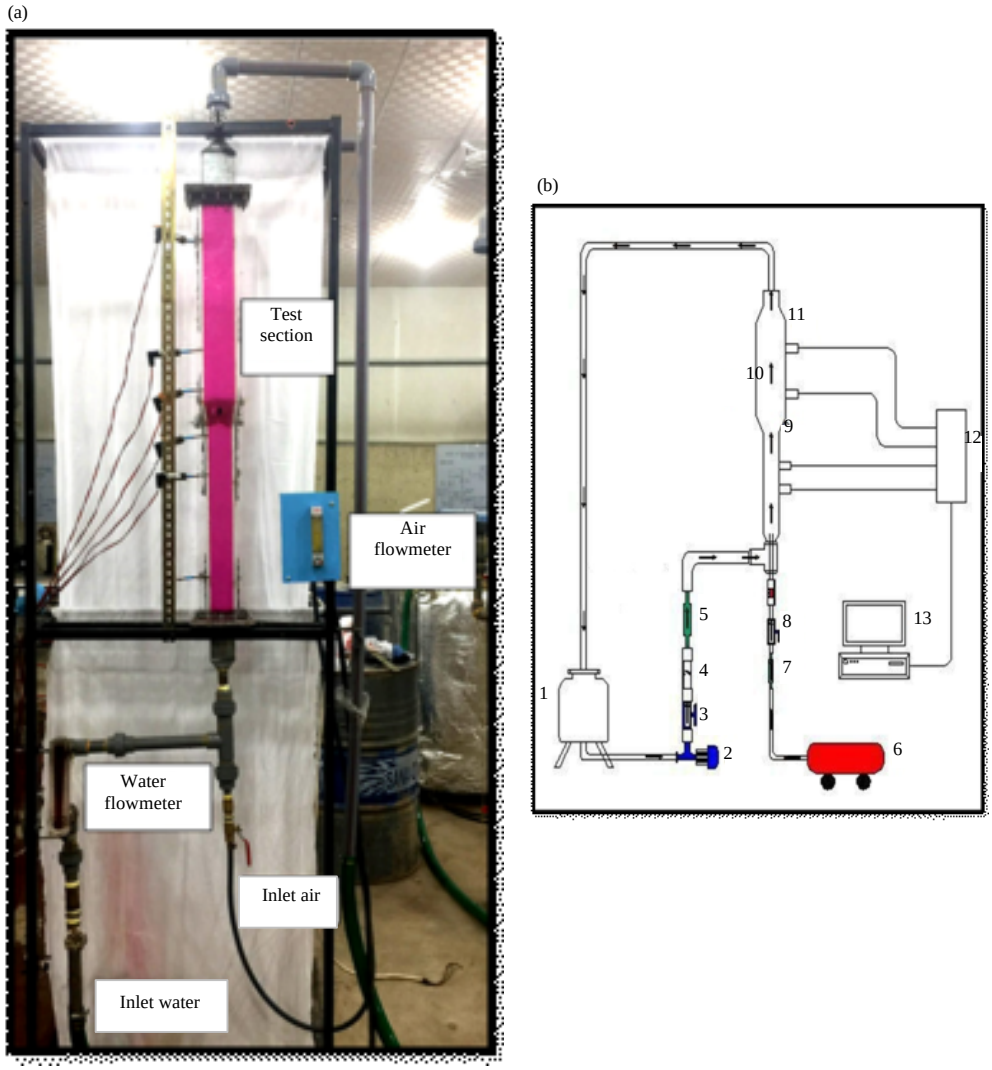

Fig. 1a: Photographic view of the experimental setup: b) Schematic diagram of the experimental setup: 1) Tank; 2) Centrifugal water pump; 3) Gate valve; 4) Check valve; 5) Water flow meter; 6) Air compressor; 7) Gate valve; 8) Check valve; 9) Air flow meter; 10) Test section; 11) Pressure sensor; 12) Pressure interface and 13) Personal computer

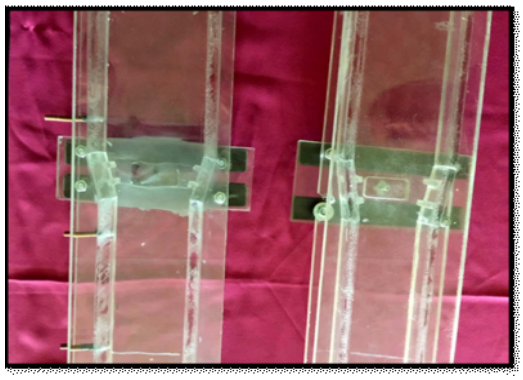

Fig. 2: Divergence sections with different opening angle

Table 1: Values of work conditions used in experiments

Qwater (L/min)	Qair (L/min)
5	5.833
15	10.833
20	16.666

thirty-six experiments were performed. All the tests were achieved by taking different values of water discharges and different values of air discharges as shown in Table 1.

- Turn on the water centrifugal pump to pump the water from the water tank
- The water valve was opened until the discharge in the flow meter reached the first value of the water discharge

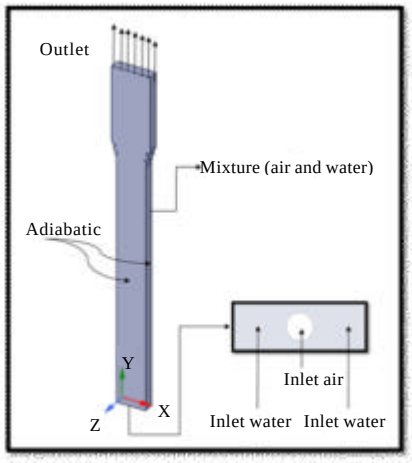

Fig. 3: Problem description

- Turn on the air compressor
- The air valve was opened until the volume rate in the flow meter reached the first value
- The pressure begging measured by the sensors located at four points along the test channel where it can be read through computer software. The image of the motion of two-phase flow was taken by Sony digital camera
- The water discharge was fixed at the first value and the air discharge was increased, until finish all the air discharges values
- Repeat all above steps with a new water discharge value, until finish all the water volume flow rate

Numerical work: For the numerical simulation, the Computational Fluid Dynamics (CFD) software has been applied for modeling water-air flow through a vertical and inclined divergence rectangular duct contains ribs, Euler Lagrange multiphase-VOF Model was used with the RNG k-ε turbulent model. The analysis and construction of the numerical field are performed in fluent (ANSYS18.0) CFD.

Geometry model: A slid work 2013 was used to draw the geometry of the system as three-dimensional structure. A circle with diameter 0.00126 m was drawn inside a rectangle in the bottom surface of the structure. So that, circle represents entry of air into the test channel and the remaining area represents the entry of water as shown in Fig. 3. All sides of the structure were set to be adiabatic walls. The bottom surface of the duct was set to represent the entry of air and water into the test channel while the top surface of the duct was set to represent the outlet flow. Description for two-phase flow can be seen from Fig. 4a, b for vertical case and Fig. 5a, b for an inclined case.

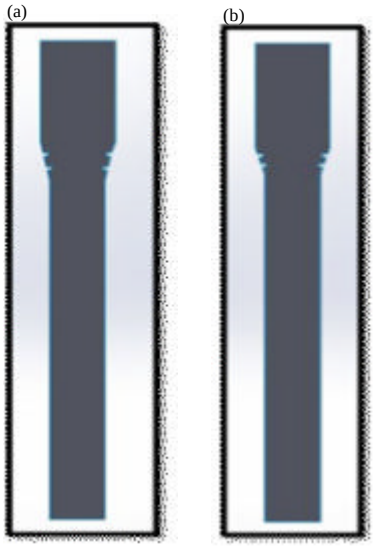

Fig. 4: Geometry for vertical case: a) $\theta = 10$ and b) $\theta = 15$

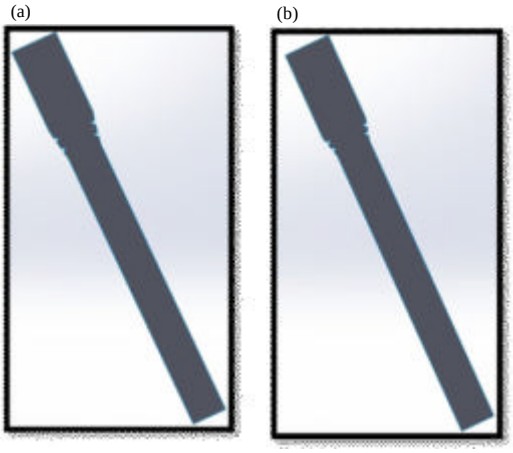

Fig. 5: Geometry for inclined case: a) $\theta = 10$ and b) $\theta = 15$

The mesh: Meshing is an important part of the numerical simulation process. The mesh influences the accuracy, convergence and speed of the solution (Bakker, 2006). The smaller elements are given more accurate results with taking into account computational cost. In this research, meshing was performed by using the Ansys Workbench 18.0 where the geometry was divided into small square elements with a size of 0.001cm for maximum and minimum. Figure 6a, b show the mesh of the two-phase flow in divergence section with 10 and 15°.

Inlet boundary condition: The air and water inlet velocity from the bottom of a duct is determined as inlet boundary condition, The superficial velocity ranges used for air and water were (0.0777-0.3108) and (0.761-2.1756 m/sec).

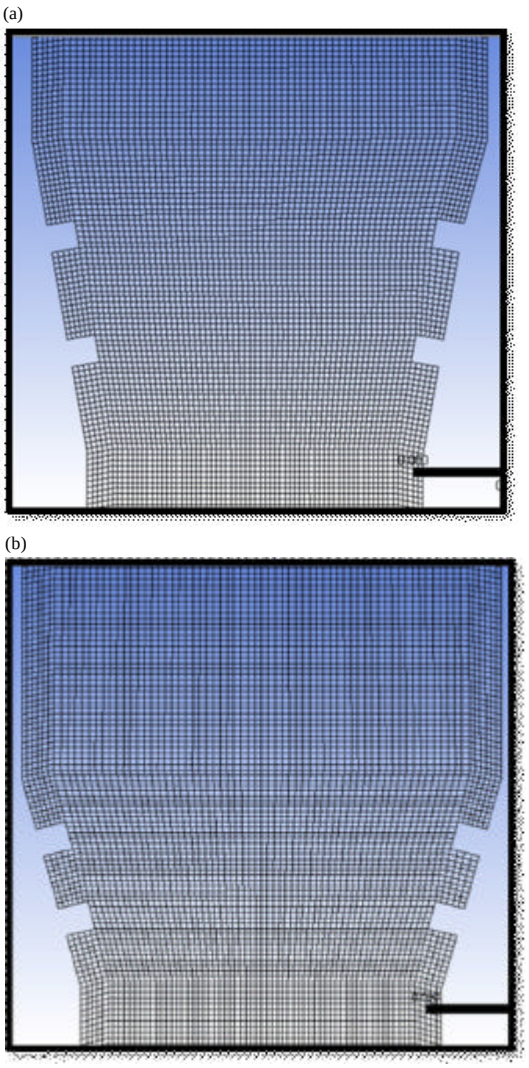

Fig. 6a): The mesh of divergence with O = 10° and b) The mesh of divergence with O = 15°

Wall boundary condition: All the portion of the channel wall was set to be adiabatic

Outlet boundary condition: The upper surface of the channel represented the exit of it and to be set as outlet flow.

Governing equations: A volume of fluid model solves the volume fraction equation and conservation equations of momentum for each phase. This model is more suitable and accurate for present work. A volume of fluid model is defined as the integration of properties of fluids in the control volume, namely the volume of a computational mesh element. The volume fraction of every fluid is tracked through every element in the computational mesh, while all fluids share a one set of momentum equations. When an element is empty with no traced fluid inside, the value of α q is zero; when the element is complete, αq = 1; and when there is a fluid interface in the element, 1>αq>1. The domain is modeled as 3-D, according to, boundary conditions of mixture internal flow and by pressure -based solver calculated a solution. The momentum equation is solved by depending on variables such as phases volume fractions and properties: density (ρ) and viscosity (μ).

The volume fraction equation: The evolution of the q-th fluid in a system on (n) fluids is governed by the transport Eq. 1:

$$\frac{\partial \alpha_q}{\partial t} + \vec{v} \cdot \nabla \alpha_q = \frac{S\alpha_q}{\rho_q} \quad (1)$$

with the following constraint:

$$\sum_{q=1}^{n} \alpha_q = 1 \quad (2)$$

By default, the source term on the right-hand side of Eq. 1 is zero but you can identify a constant or user-defined mass source for each phase. For every element, the Characteristics of mixture like dynamic viscosity and mixture density are based on the volume fraction of all phases as given by Eq 3.

$$\rho = \sum \alpha_n \rho_n ; \mu = \frac{\sum \alpha_n \rho_n \mu_n}{\sum \alpha_n \rho_n} \quad (3)$$

The momentum equation: one momentum equation is resolved during the field and the resulting velocity field is shared among the phases. The momentum equation, shown below is based on the volume fractions of all phases through the characteristics of ρ and μ.

$$\frac{\partial}{\partial t}\left(\rho \vec{v}\right) + \nabla \cdot \left(\rho \vec{v} \vec{v}\right) = -\nabla p + \nabla \cdot \left[\mu\left(\nabla \vec{v} + \nabla \vec{v}^{\wedge T}\right)\right] + \rho \vec{g} + \vec{F} \quad (4)$$

Where

$\vec{v}$ = Velocity field and

$\vec{F}$ = A body force

Turbulence model: ANSYS Fluent 18.0 presents three approaches for the k-Epsilon turbulence model in the multiphase flow:

- Turbulence mixture model
- Turbulence dispersed model
- Turbulence model for each phase

Turbulence RNG mixture model was set for the two-phase flow model which can be defined through these equations (Fluent User's Guide).

ANSYS:

$$\frac{\partial}{\partial t}(\rho_m K)+\nabla\cdot\left(\rho_m \vec{V}_m \in\right)=\nabla\cdot\left(\frac{\mu t.m}{\sigma K}\nabla K\right)+G_{K.m}-\rho_m \in \quad (5)$$

$$\frac{\partial}{\partial t}(\rho_m \in)+\nabla\cdot\left(\rho_m \vec{V}_m \in\right)=\nabla\cdot\left(\frac{\mu t.m}{\sigma K}\nabla \in\right)+\frac{\in}{K}\left(C_{1\in}C_{K.m}-C_{2\in}\rho_m \in\right) \quad (6)$$

Where

k = Turbulent kinetic energy
$\in$ = The turbulent dissipation rate
G = The energy
σ = The turbulent Prandtl number for k and $\in$

The density and the velocity of the mixture can be found by using Eq. 7 and 8, respectively:

$$\rho_m=\sum_{i=1}^{N}\alpha_i\rho_i \quad (7)$$

$$\vec{V}_m=\frac{\sum_{i=1}^{N}\alpha_i\rho_i\vec{V}_i}{\sum_{i=1}^{N}\alpha_i\rho_i} \quad (8)$$

The turbulent viscosity and kinetic energy of the mixture can be found by using Eq. 9 and 10, respectively:

$$\mu_{t.m}=\rho_m C_m\frac{K^2}{\in} \quad (9)$$

$$G_{K.m}=\mu_{t.m}\left(\nabla\vec{V}_m+\left(\nabla\vec{V}_m\right)^T\right):\vec{V}_m \quad (10)$$

The model constants can be seen in Table 2:

RESULTS AND DISCUSSION

Experimental results

Effect of water and air discharge on pressure profile: Figure 7 and 8 show the effect of increasing water and air

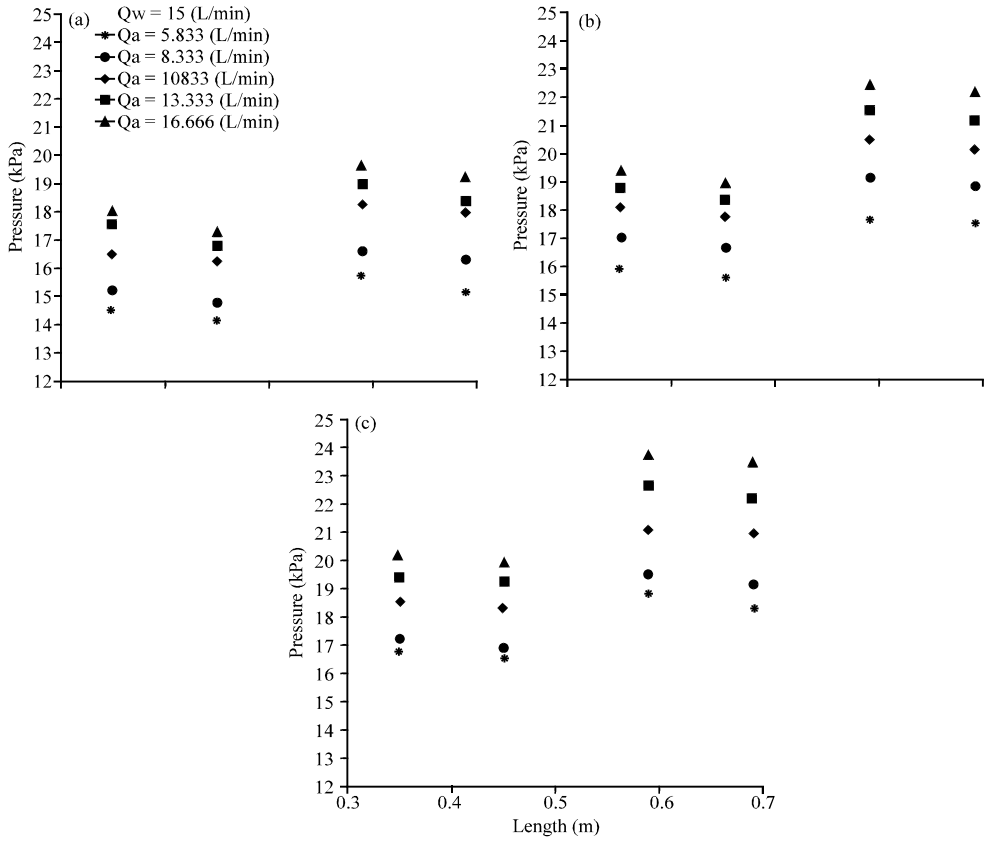

Fig. 7: Effect water discharge on pressure profile for opening angle 10° (vertical)

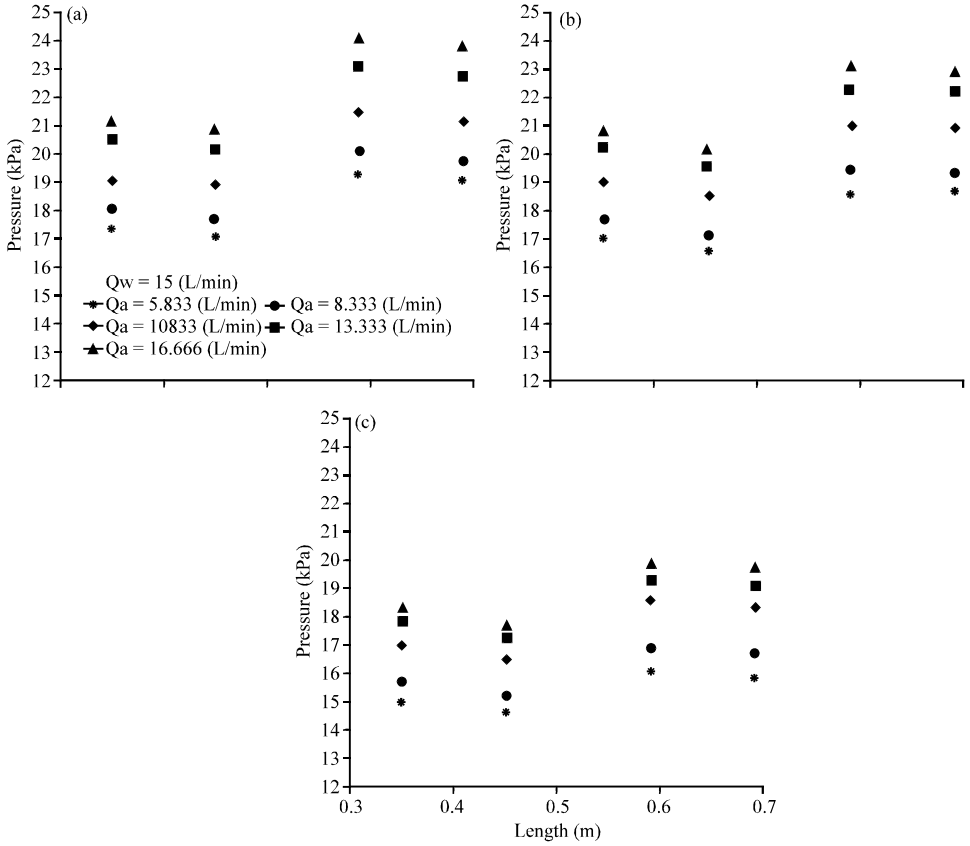

Fig. 8: Effect water discharge on pressure profile for opening angle 15° (vertical)

Table 2: Model constants

The constant	Value
C_m	0.09
C_1-Epsilon	1.44
C_2-Epsilon	1.92
σ	1.00
σ_ε	1.30

discharge on the experimental results of the pressure profile at four different points along the test channel. Note from these figures that the value of the mixture is progress the flow. When the mixture reaches the divergence section, the pressure value begins to increase. At the upstream of the divergence study, the pressure value will decrease again. It can be seen that the pressure profile increased with increasing water or air discharge because to the volume of the test channel was constant and it was already occupied by the air and water, so, any increase in the amount of water or air would increase the pressure over the walls of the channel.

Effect of water and air discharge and opening angle on the recovery pressure: Figure 9-12 show the experimental results for the recovery pressure through the vertical divergence section with different air and water discharge. It can be concluded from these figures that the recovery pressure increases with increasing discharge of air or water for both the 10 and 15 opening angles. It was observed, too that the recovery pressure for the opening angle 15 is less than the recovery pressure at the opening angle 10 at the same air and water discharge because of the presence of the additional flow area for case of angle 15° which production more turbulence wherefore more eddies are generated, leading to make the recovery pressure less than the case of opening angle of 10°.

Numerical results: The purpose of the numerical CFD to study the pressure distribution and air volume fraction distribution through ribs divergence section for a vertical and inclined position. As like as the experimental study, a region of a test is in between sensor 1 and 4. Figures 13-18 show the contours of pressure distribution for two-phase flow through vertical and inclined ribs divergence test channel with opening angle 10°, at various values of water and air.

Comparison between experimental and numerical Effect of water and air discharge on pressure profile: Observed that behavior of effect of increasing the

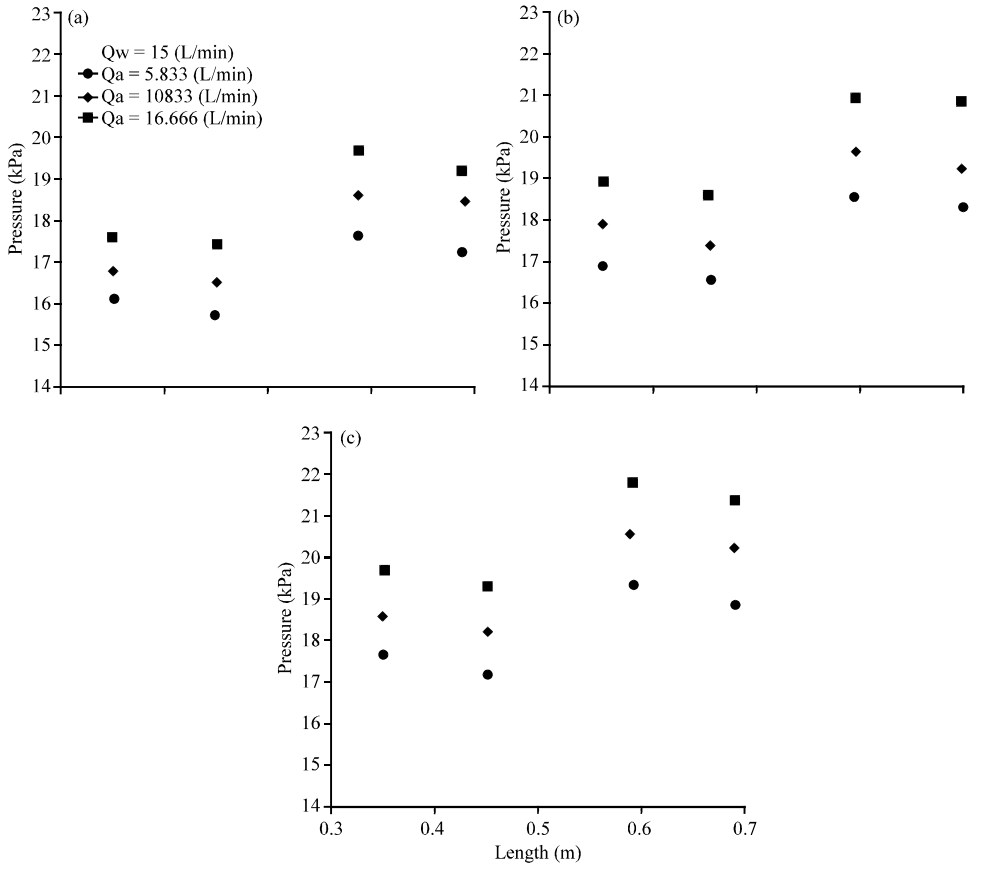

Fig. 9: Effect water discharge on pressure profile for opening angle 10° (inclined)

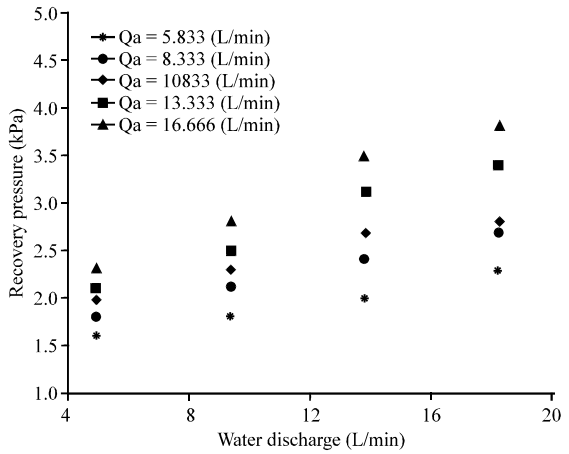

Fig. 10: Recovery pressure for different values of water discharge at opening angle 10° (vertical)

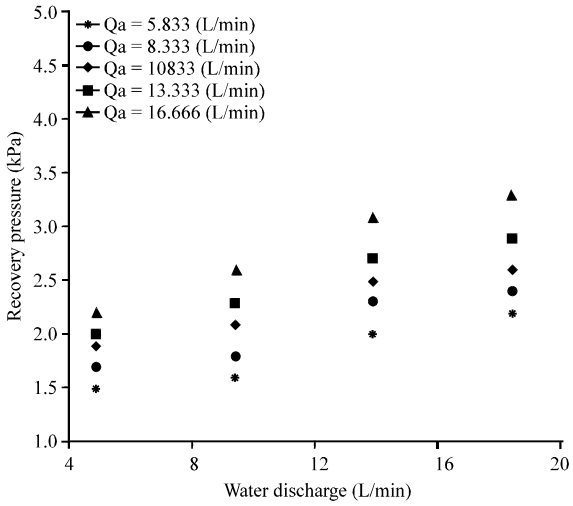

Fig. 11: Recovery pressure for different values of water discharge at opening angle 15° (vertical)

discharge of air or water on pressure distribution was similar for experimental and numerical work. As observed that the values of experimental and numerical results were close and the maximum deviation was (7%). It was also, observed that the numerical results were greater than the results of the experimental result due to neglect of several

effects such as neglect of the turbulence caused by the pump and neglect of the effect of sharp edges of enter the air and water on the pressure and also neglect friction between the mixture and the walls of the channel. Figure 19 demonstrates the compression between effect of increasing water discharge on the experimental and numerical results of the pressure profile at four different points along the vertical test channel with opening angle 10 for various values of air discharges (5.833,10.833 and 16.666).

The influence of water and air discharge on the flow behavior: Figure 20 and 21 demonstrate the experimental flow behavior through the photos that were taken for ribs

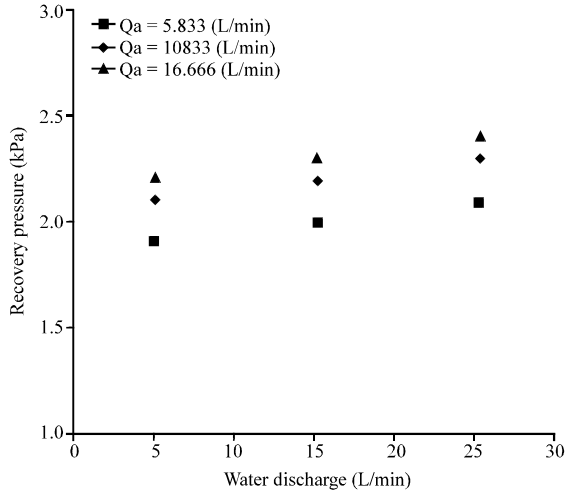

Fig. 12: Recovery pressure for different values of water discharge at opening angle 10° (inclined)

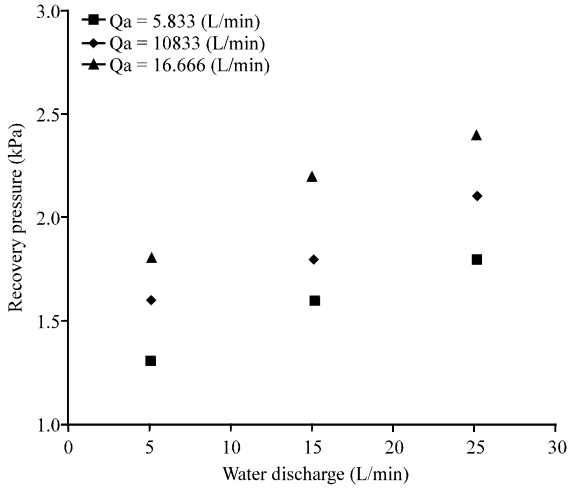

Fig. 13: Recovery pressure for different values of water discharge at opening angle 15° (inclined)

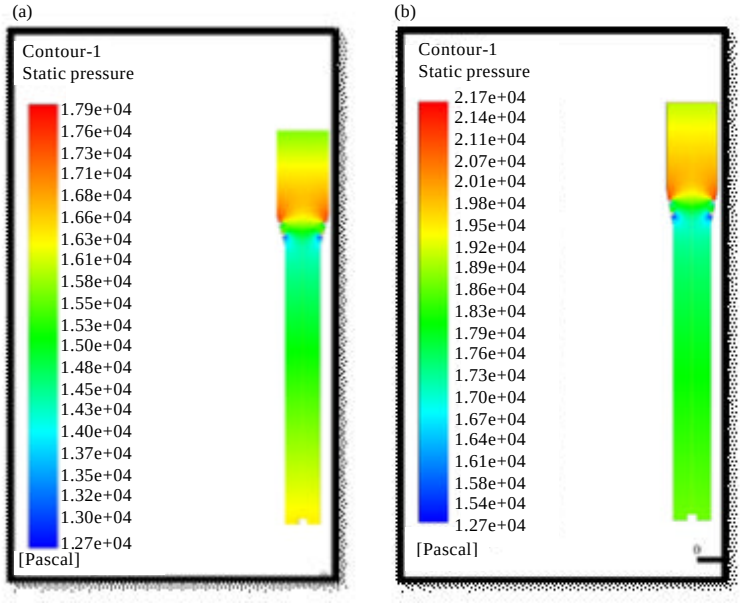

Fig. 14: Effect of air discharge on pressure distribution at 5 L/min water discharge (opening angle10°): a) Q air = 5.833 L/min and b) Q air =16.666 L/min

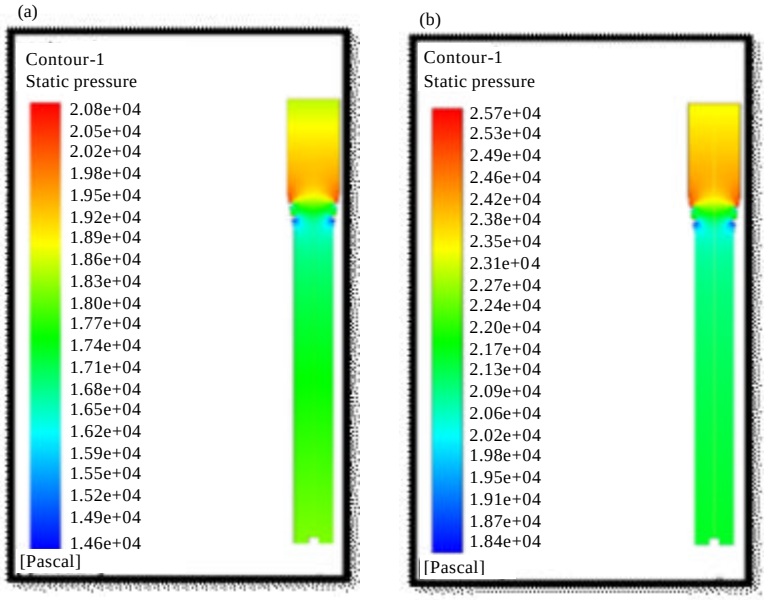

Fig. 15: Effect of air discharge on pressure distribution at 20 L/min water discharge (opening angle10°): a) Q air = 5.833 l/min and b) Q air = 16.666 l/min

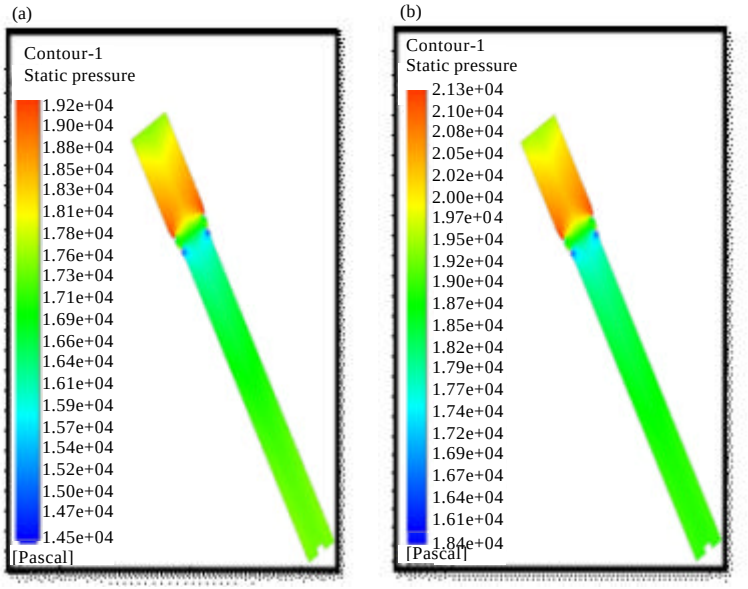

Fig. 16: Effect of air discharge on pressure distribution at 5 L/min water discharge (opening angle10°): a) Q air = 5.833 l/min and b) Q air = 16.666 L/min

divergence section and compared it with the contour of air volume fraction which obtained by numerical simulation.A nearby similarity for the behavior of flow between the experimental photos and the images of air volume fraction found with ANSYS 18.

Comparison the pressure values between the vertical and inclined flow: When comparing the experimental and numerical values of pressure for case of vertical flow against inclined flow, observed that the pressure values for case of vertical flow are higher than the inclined flow case of both the experimental and the numerical values because, for the case of vertical flow, the column of the mixture is higher for vertical flow case than inclined flow at same location of pressure transducer. Figure 22 illustrates a comparison between the values of the experimental and numerical pressure between the state of the vertical and the inclined flow at the value of the discharge of water 5 L/min and different air discharge.

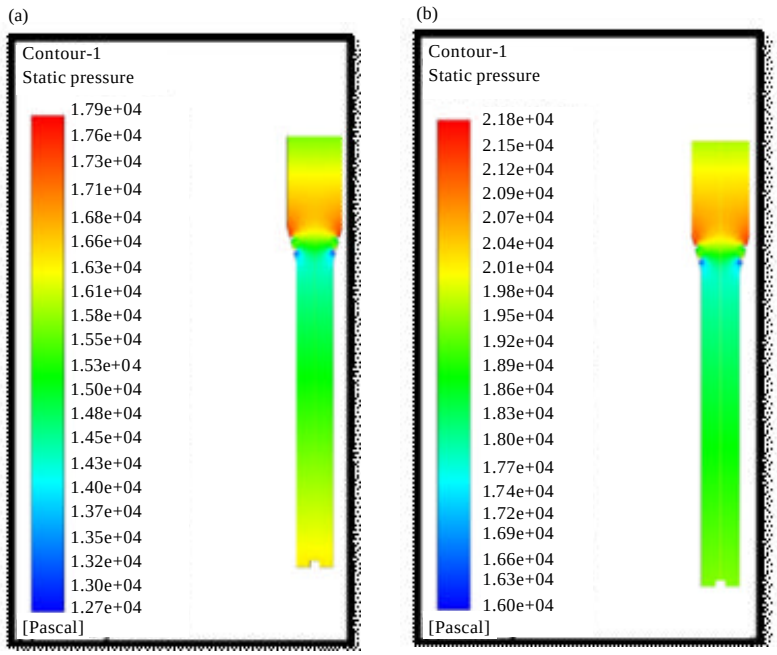

Fig. 17: Effect of air discharge on pressure distribution at 5 L/min water discharge (opening angle 15°): a) Q air = 5.833 L/min and b) Q air = 16.666 L/min

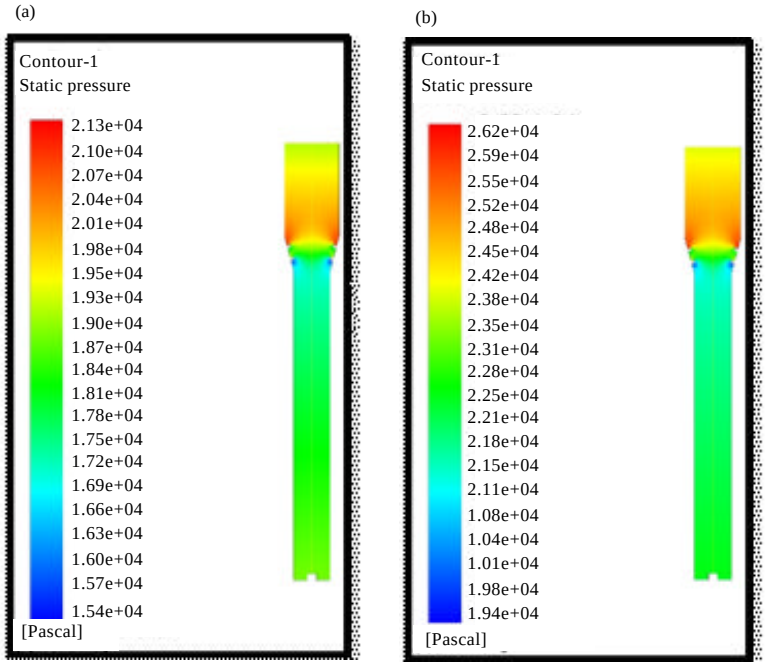

Fig. 18: Effect of air discharge on pressure distribution at 20 l/min water discharge (opening angle15°): a) Q air =5.833 L/min and b) Q air =16.666 L/min

Visualization flow pattern: By observing the flow during the vertical and inclined divergence test section, we observe that the current flow pattern at the downstream and upstream for the divergence study is the slug flow

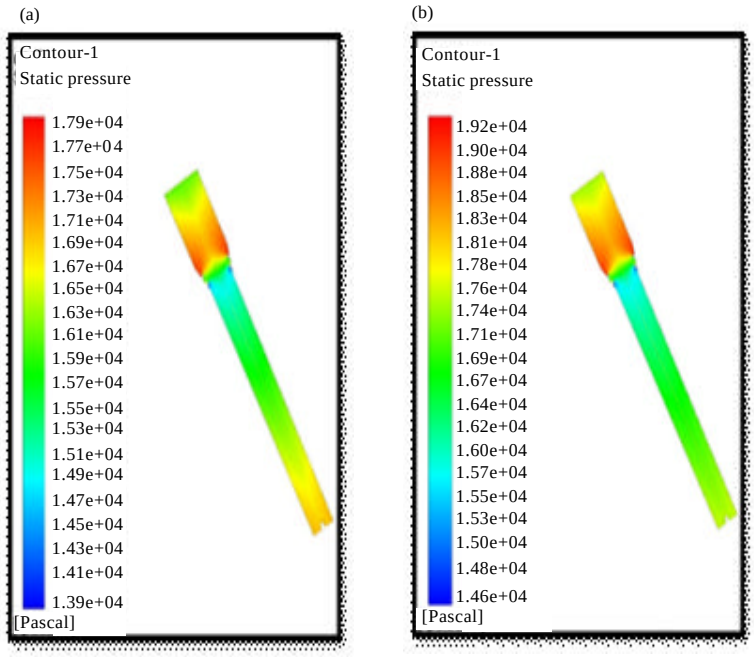

Fig. 19: Effect of air discharge on pressure distribution at 5 L/min water discharge (opening angle15°): a) Q air = 5.833 L/min and b) Q air = 16.666 L/min

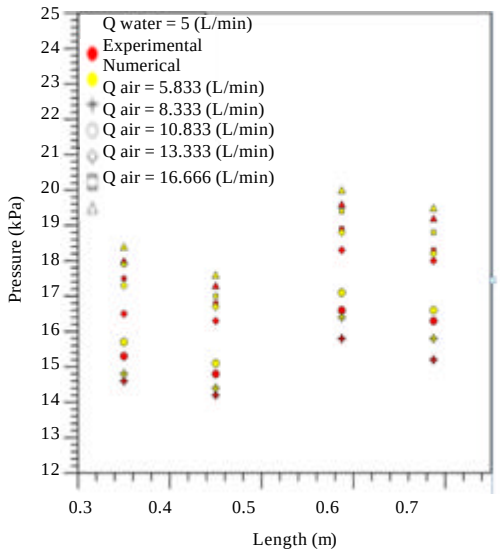

Fig. 20: Compression between effect water discharge on Experimental and numerical pressure profile for opening angle 10° (vertical): a) Q air = 5.833 l/min and b) Q air = 16.666 L/min

while the flow pattern through the divergence section can not be determined due to the high disturbance caused by the mixing of the phases due to the presence of the ribs in particular when air or high water discharge as shown in Fig. 23 and 24.

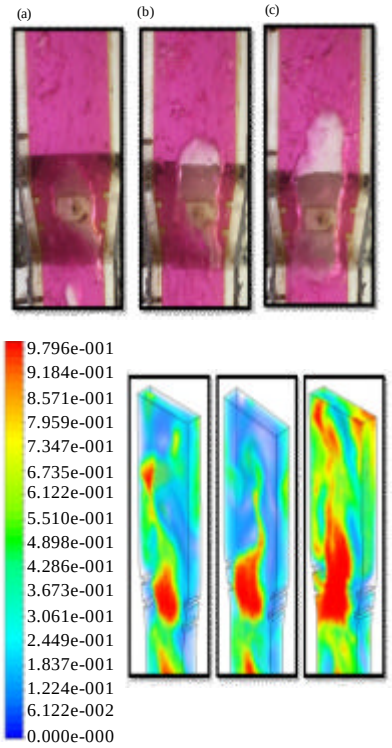

Fig. 21: Compression between effect water discharge on Experimental and numerical pressure profile for opening angle 10° (vertical): Q air a) 5.833; b) 10.833 and c) 16.666

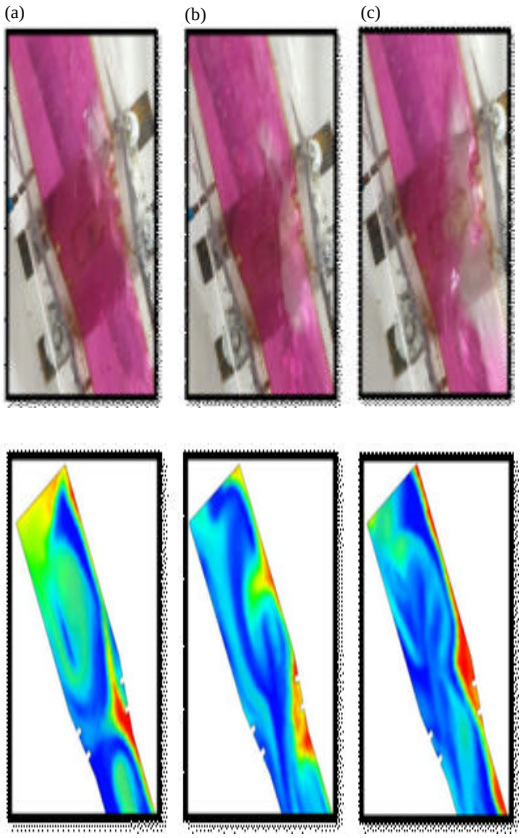

Fig. 22: Compression between the experimental and numerical of effect of air discharge on the flow behavior at Q water = 5 L/min with opening angle =10° (inclined): Q air a) 5.833; b) 10.833 and c) 16.666

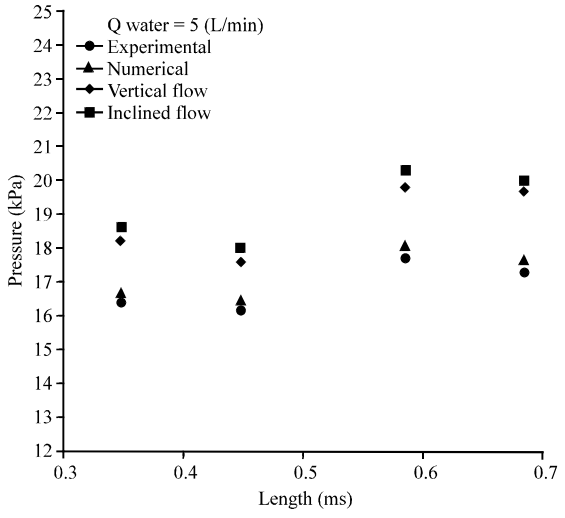

Fig. 23: Comparison the pressure values between the vertical and inclined flow

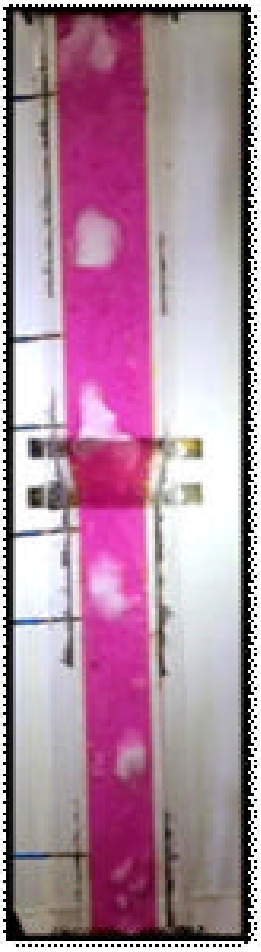

Fig. 24: flow pattern in vertical channel

Fig. 25: Flow pattern in inclined channel

CONCLUSION

When water discharge increases, the pressure recovery rises as when air water discharge increases, the pressure recovery increases by. When the opening angle increases, the pressure recovery decreases due to the losses caused by eddies being stronger. When air discharge increases, the volume and amount of bubbles increases. Also as continuous air discharge increases, flow turbulence increases as does the velocity of generating eddies. The volume of bubbles decreases when water discharge increases. Also, as continuous water discharge increases, the flow is more turbulent and unstable and eddies are stronger. The effect of increases of water discharge on the turbulence is higher than the effect of increases of air discharge because the water density is higher and thus, the inertia force is greater for the case of water.

NOMENCLATURE

S = Source term, dimensionless
P = Pressure (kPa)
g = Acceleration gravity (m/sec^2)

Greek symbols:
θ = Divergence opening angle
α = Volume fraction
ρ = Density (kg/m^3)
μ = Dynamic viscosity (kg/msec)
Δ = Difference
K = Turbulence kinetic energy (m^2/sec^2)
ϵ = Turbulence kinetic energy dissipation rate (m^2/sec^2)

Subscripts:
n = Number of phase
q = Phase
m = Mixture

REFERENCES

Abadie, T., J. Aubin, D. Legendre and C. Xuereb, 2012. Hydrodynamics of gas-liquid Taylor flow in rectangular microchannels. Microfluid. Nanofluid., 12: 355-369.

Abdelall, F.F., G. Hahn, S.M. Ghiaasiaan, S.I. Abdel-Khalik and S.S. Jeter *et al*., 2005. Pressure drop caused by abrupt flow area changes in small channels. Exp. Therm. Fluid Sci., 29: 425-434.

Abed, E.M. and R.S. Al-Turaihi, 2013. Experimental investigation of two-phase gas-liquid slug flow inclined pipe. J. Univ. Babylon, 21: 1579-1591.

Ahmadpour, A., S.M.N.R. Abadi and R. Kouhikamali, 2016. Numerical simulation of two-phase gas-liquid flow through gradual expansions-contractions. Intl. J. Multiphase Flow, 79: 31-49.

Ahmed, W.H., C.Y. Ching and M. Shoukri, 2008. Development of two-phase flow downstream of a horizontal sudden expansion. Intl. J. Heat Fluid Flow, 29: 194-206.

Ahmed, W.H., C.Y. Ching and M. Shoukri, 2007. Pressure recovery of two-phase flow across sudden expansions. Intl. J. Multiphase Flow, 33: 575-594.

Anupriya, S. and S. Jayanti, 2014. Experimental and modelling studies of gas-liquid vertical annular flow through a diverging section. Intl. J. Multiphase Flow, 67: 180-190.

Bakker, A., 2006. Applied computational fluid dynamics, mesh generation, computational fluid dynamics lectures. Fluent Inc., Pennsylvania, USA.

Behzadi, A., R.I. Issa and H. Rusche, 2004. Modelling of dispersed bubble and droplet flow at high phase fractions. Chem. Eng. Sci., 59: 759-770.

Brankovic, A. and I.G. Currie, 1996. Turbulent two-phase flow through a sudden pipe expansion: LDA experiments and CFD predictions. Intl. J. Comput. Fluid Dyn., 6: 189-205.

Chen, I.Y., C.C. Liu, K.H. Chien and C.C. Wang, 2007. Two-phase flow characteristics across sudden expansion in small rectangular channels. Exp. Therm. Fluid Sci., 32: 696-706.

Chen, I.Y., M.C. Chu, J.S. Liaw and C.C. Wang, 2008. Two-phase flow characteristics across sudden contraction in small rectangular channels. Exp. Therm. Fluid Sci., 32: 1609-1619.

Eskin, N. and E. Deniz, 2012. Pressure drop of two-phase flow through horizontal channel with smooth expansion. Proceedings of the International Conference on Refrigeration and Air Conditioning, July 16-19, 2012, Purdue University Press, West Lafayette, Indiana, USA., pp: 1-10.

Kondo, K., K. Yoshida, T. Matsumoto, T. Okawa and I. Kataoka, 2002. Flow patterns of gas-liquid two-phase flow in round tube with sudden expansion. Proceedings of the 10th International Conference on Nuclear Engineering Vol. 3, April 14-18, 2002, American Society of Mechanical Engineers, New York, USA., pp: 179-186.

Kourakos, V.G., P. Rambaud, S. Chabane, D. Pierrat and J.M. Buchlin, 2009. Two-Phase Flow Modelling Within Expansion and Contraction Singularities. In: Computational Methods in Multiphase Flow V, Mammoli, A.A. and C.A. Brebbia (Eds.). WIT Press, Southampton, England, pp: 27-43.

Roul, M.K. and S.K. Dash, 2011. Two-phase pressure drop caused by sudden flow area contraction/expansion in small circular pipes. Int. J. Numer. Methods Fluids, 66: 1420-1446.

Sakr, I.M., W.A. El-Askary, A. Balabel and K. Ibrahim, 2012. Computations of upward water-air fluid flow in vertical pipes. CFD. Lett., 4: 193-213.

Ueda, Y., T. Nakajima, T. Ishii, R. Tsujino and M. Iguchi, 2012. Numerical simulation of gas-liquid two-phase flow in a horizontally placed hydrophobic rectangular channel (Part 1, Influence of Abrupt Expansion). High Temp. Mater. Proc., 31: 405-410.

Wang, C.C., C.Y. Tseng and Y. Chen, 2010. A new correlation and the review of two-phase flow pressure change across sudden expansion in small channels. Intl. J. Heat Mass Transfer, 53: 4287-4295.